07

Mechanism of local damage to photovoltaic cells by geomagnetic plasma electrons

© V.M. Zykov, K.E. Evdokimov, D.A. Neyman, A.M. Vladimirov, G.A. Voronova

Tomsk Polytechnic University, 634050 Tomsk, Russia e-mail: evdokimov@tpu.ru

Received July 19, 2024 Revised December 28, 2024 Accepted March 10, 2025

With regard to the initial period of active existence of a spacecraft (SC), the processes of anomalous degradation of the power of InGaP/InGaAs/Ge photovoltaic cells (PVC) were experimentally studied during bench tests for the effect of geomagnetic plasma by modeling the electron component of the plasma taking into account the periodic intersection of the SC orbit with the Earth's radiation belt, including the auroral zone. Using the methods of video recording of electroluminescence and measuring dark I-V curves under bench conditions, as well as the methods of microscopy, absolute spectrometry of electroluminescence and dark I-V curves after the end of bench tests, the processes of anomalous degradation of PVC were established, occurring with the participation of technological microdefects of the surface and microbreakdowns of the cover glasses of K-208. A phenomenological impact mechanism of anomalous accelerated degradation of the power of PVC at the initial stage of the SC existence is proposed. The highest rate of anomalous power degradation is observed for solar cells with technological defects in p-n-junctions.

Keywords: solar panels of spacecraft, geomagnetic plasma, anode-initiated flashover, bulk microbreakdown of dielectric, damage to photovoltaic device.

DOI: 10.61011/TP.2025.07.61460.236-24

Introduction

As it is known, degradation of power of photovoltaic cells (PVC) of solar panels (SP) in conditions of near-Earth space depends on an orbit type. Thus, for example, at the GPS global navigation system's orbit anomalous decrease of the SB power during the term of active existence of a spacecraft (SC) can in several times exceed estimates of power current degradation based on the modern space models, which are well-established for the orbits like the geostationary one [1,2]. In particular, true degradation of SP power of the GPS SVN 41 satellite was 30% for 9 years, while the estimate done by means of the AE8MAX model yields decrease of the SP power for at most 12% [1].

At the same time, the rate of anomalous degradation of SP power at the GPS global navigation system's orbit is maximum at the initial period of time, decreases with increase of an integral flux of electrons and protons of the geomagnetic plasma during orbit operation and is almost independent of a phase of solar activity. Such kinetics of the SP PVC power indicates that degradation is mainly due to PVC defects of technological origin, rather that defects that appear during operation. Taking this into account as well as a difference of the orbits of the GPS system and the geostationary orbit, it can be assumed that the main reason of anomalous degradation of SP power might be related to specific features of a defect state of cover glasses and PVC semiconductor structures as well as to the fact that the

orbit is characterized by periodically intersecting the Earth's radiation belt.

Based on results of many ground-based tests of the SP samples affected by protons and electrons of the geomagnetic plasma, the following was established:

- Contribution by protons of the geomagnetic plasma to spacecraft electrization plays a secondary role in relation to electron effect [3]. Nevertheless, the proton flux can significantly affect both a surface charge state due to initiation of electron emission and a structure of a glass surface layer [4], resulting to formation of gas-filled bubbles as well [5].
- At the end of the period of spacecraft active existence, contribution of radiation-induced defects to reduction of optical transparence of the PVC radiation-resistant cover glasses of the grade K-208 and CMG is about 1% [6,7].
- Under effect of the geomagnetic plasma electron fluxes the surface of the PVC cover glasses is modified by electrical-discharge processes, and if the SC orbit-averaged electron fluxes are used in the tests, then in this case variation of the PVC power does not exceed several percent [6].
- The PVC cover glasses exhibit separate local microbreakdowns of a depth of up to the complete thickness of the glass [6], which are sources of generation of electrical-discharge plasma as well as sources of periodic generation of shock waves affecting the PVC semiconductor heterostructure.

- Through microbreakdowns of the protective glass are characterized by radial microcracks [7,8], while some microbreakdowns are intersected by long cracks in the glass [8].
- Electrostatic discharges (ESD) can result in deposition of the electrical-discharge plasma material to the surface of the cover glass and subsequent reduction of transparency and power drop [2].

Let us note that the factors mentioned in the abovelisted papers first of all affect the characteristics of the cover glasses, and their influence in proportion to an integral flux of charged particles, therefore, will provide the SP power degradation rate close to the constant value. As shown in the study [1], this degradation rate is really close to the constant, but only at the mid- and the final-stage of SC active existence. At the same time, the initial stage is characterized by an increased power degradation rate, and presently there is no commonly-accepted model explaining it. Thus, the SP voltage and current degradation rate at the GPS orbit was explained in the study [9] by using a new three-dimensional NASA model for the daily-mean radiation-belt electron flux (RB-Daily-E), which covers 25 differential energies within the range (33-7700 keV), 17 inclination angles and a variable number of shells L from 2 to 7. The modelled degradation of the SP voltage well complied with telemetry data at the GPS orbit. On the other hand, using this model resulted in significant underestimation of the SP current degradation rate. These results made the authors of the paper [9] to conclude that the daily-mean electron flux is a main factor of SP voltage degradation, while the SP current degradation is affected by other factors. In our assumptions, one of these factors may be not the daily-mean electron flux, but rather a fluence and a density of the electron flux that are observed in conditions when the SC orbit intersect the Earth's radiation belt.

The present study was aimed at establishing causes of anomalous degradation of the SP PVC power at the orbits with the periodic intersection with the Earth's radiation belt, including the auroral subpolar zone. In this case "anomalous" means accelerated power degradation at the initial stage of SC existence. It has considered estimate of contribution to this degradation of damage to the photovoltaic device by shock mechanical effects which appear during the electrostatic discharges along the surface and in channels of the through microbreakdowns of the cover glass. A role of initial imperfection of the cover glasses and the PVC semiconductor structure has been studied.

Ground-based modeling of effect of geomagnetic plasma on SP PVC

In the ground-based conditions, a mechanism of accelerated initial anomalous degradation of SP power manifested itself in the test bench "Prognoz-2" [10] when modeling effect of the geomagnetic plasma electrons on the SP sample (the electron energy of 40 keV, the current density of

10 nA/cm²) taking into account electron fluence collection exclusively by periodic intersection with the subpolar auroral zones by the SC at the polar orbit of the altitude of 800 km. During the accelerated tests of the SP sample, the time of SC staying in the auroral zone was overestimated in 6-8 times (2 min instead 15-20 s), while the temperature mode (−65 °C) corresponded to the worst-case scenario when the SP PVCs are in the FC shadow. The collected electron fluence was $1.5 \cdot 10^{15} \, \text{cm}^{-2}$. For reliable estimate of the SP operating current degradation rate, the number of modeled intersections of the SC orbit wit the auroral zones at the North and South poles of the Earth, for the most dangerous temperature mode (-65 °C), was selected to be 100 (25 SC revolutions around the Earth). The SP sample consisted of the PVCs based on the InGaP/GaAs/Ge heterostructure with the nominal sizes $40 \times 80 \,\mathrm{mm}$, which are formed in rows (strings) of serial elements, and was oriented perpendicular to the electron flux. The PVC cover glasses were manufactured of the K-208 optical glass of the thickness of $130 \,\mu\text{m}$.

The manufacturer of the SP sample has measured characteristics of 20 PVCs of the panel, for which the current value was recorded in an operating point before and after the tests. At least one PVC has shown reduction of the operating current by 72% from 480 to 136 mA, so have at least three samples by 6-10%, at least five samples were characterized by drop 1-3%, and at least six samples were not changed whatsoever.

After completion of the tests, some PVCs of the SP sample were studied by measuring dark current-voltage curves (I-U curves) and photodetection of electroluminescence (EL) when applying direct electric displacement. The EL spectra of some PVCs were studies by means of the spectrophotometer Avantes Avaspec 2048. The dark I-U curves, photo images of EL distribution along the surfaces of the PVC samples as well as the EL spectra are shown on Fig. 1.

The EL spectrum of multi-junction PVCs is characterized by several intensity peaks, which occur in interband radiative recombination of the charge carriers, whereas the peak position is determined by a band gap width of the respective p-n-junction [11]. In particular, for the PVCs based on the InGaP/GaAs/Ge heterostructure, the sensitivity range of matrices of common image cameras includes radiation bands of the p-n-junctions based on InGaP and GaAs with the maximums 660 and 900 nm, respectively. Radiation of the Ge p-n-junction is further inside the IR region and it is not recorded by such instruments. Usually, the spectral sensitivity of the camera around 660 nm is higher than around 900 nm [12]. So, local enlargement of the 660 nm peak might look like a bright spot even with general reduction of the EL light flux.

EL of the defect state of the semiconductor structure of the PVCs (which had been previously tested for effect by the electron component of the geomagnetic plasma with modeling the periodic intersection of the Earth's radiation belt) has been controlled by the method of absolute

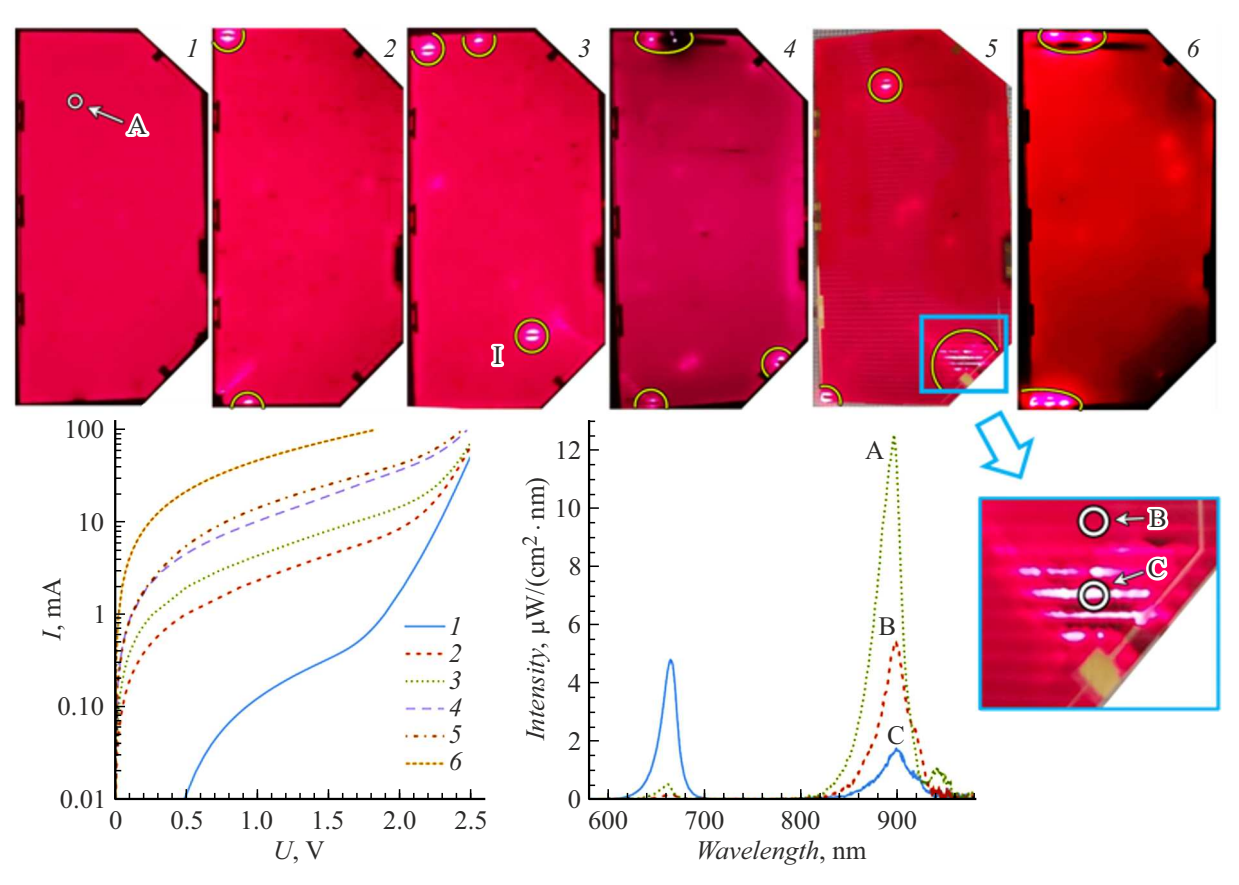


Figure 1. Photo images (above), the dark I-U curves (bottom left) and the PVC EL spectra (below in the middle) after irradiation with an electron beam. The samples and the respective I-U curves are numbered from *I* to *6*. The EL spectra and their recording positions are marked with the letters "A", "B" and "C". I marks an area of studying the short-circuit current density.

spectrometry to show that, on one hand the EL output is distributed quite uniformly across the larger part of the area of each sample, whose average value can be assumed to be an EL basic level of the sample. On the other hand, some PVCs have local places of anomalous absolute EL output at the wavelength of 660 nm, which in calculation per a unit area exceeds the averages basic value, but at the same time the absolute EL output at the wavelength of 900 nm is significantly reduced. For illustration, Fig. 1 shows the EL spectra in the points "A", "B" and "C", which are located on the least damaged PVC (the sample $N_{\underline{0}}$ 1), in the vicinity of the area of anomalous EL of the damaged PVC and inside it (the sample N_0 5), respectively. This ratio of intensities of the EL peaks indicates local redistribution of electric voltage between the p-n-junctions of the photostructure in favor of the upper InGaP-based junction due to stron local damage of the middle GaAs-based p-n-junction and reduction of respective parallel resistance. The reduced EL output of the (partially-) shunted p-n-junction and increased output for the other junctions are also reported in the paper [13].

These local circuit shortings provide significant current growth in the PVC dark I-U curves and this current growth correlates with the number of PVC locations with anomalously high absolute EL output at the wavelength of

660 nm. Fig. 1 marks these locations with yellow ellipses and has the samples numbered in accordance with growth of the number of visible areas of local shunting from 0 for the sample N_2 1 to 5 for the PVC N_2 6. We note that at least two samples — N_2 4 and N_2 5 — after irradiation have undergone reduction of the operating current by 10% and 6%, respectively (the data for the other samples were not recorded by the manufacturer).

Some PVCs have exhibited special areas that are characterized by increased EL output in the visible range at the quite large area. These areas are adjacent to primary microbreakdowns of the cover glass and consist of the glass crack network with many microbreakdowns where the cracks are intersected by grid electrodes, whose edges are concentrators of the electric field. The PVC containing the area with the high density of the microbreakdowns is exemplified on Fig. 1 (the sample N_2 5 and its enlarged Another example is shown on Fig. 2, b, whose one photo reveals a microscope image of the EL output anomalous location at the wavelength of 660 nm and the area of the glass crack network, which is identified by additional illumination. It follows from comparing the dark I-U curves for the PVCs № 4 and № 5 in the Fig. 1 that contain the same number of the locations of anomalous EL

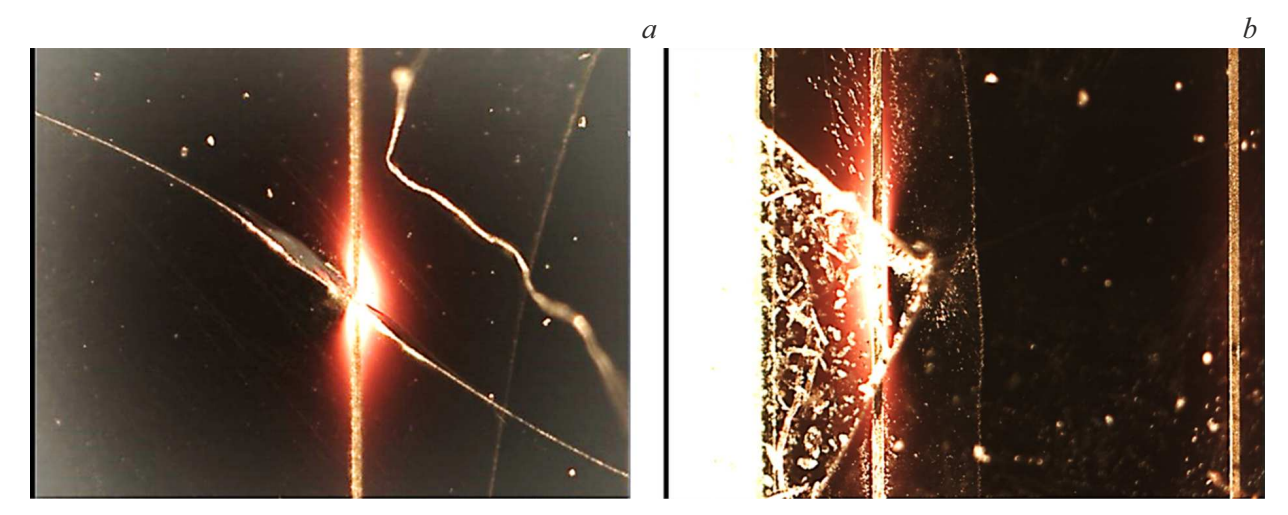


Figure 2. Micro-photoimages of locations of anomalous EL output, which are accompanied by the through breakdown and a single crack (a), several breakdowns and a crack network (b).

output at the wavelength of 660 nm (that differ by a special area with the network of cracks and microbreakdowns) that there is a relation between significant increase of the current of the dark I-U curve and formation of such areas.

By the microscope method with illumination, it was found that the local locations of anomalously high EL output at the wavelength of $660 \,\mathrm{nm}$ were accompanied with through microbreakdowns and glass cracking (Fig. 2). Such microbreakdowns and cracks of the cover glass, which occurred after irradiation by the electron beam modeling effect of the geomagnetic plasma and were accompanied by degradation of one of the p-n-junctions of the PVC, were also observed in the study [8].

In order to clarify the PVC damage mechanism, an additional test of another SP sample was performed and the PVC was investigated as per the above-described technique. This test included video recording of ESD on the PVC surface. Besides, the Flir A325sc thermal imager was used to measure temperature distributions along the surface of the PVC samples being electrically displaced. Fig. 3 shows a sequence of photo images of EL, ESD and temperature distribution, which demonstrates appearance of a local shunt during irradiation by the electron beam.

The EL output distribution before irradiation (Fig. 3, a) is quite uniform. At the initial stages of irradiation, the ESDs start at the sample edges (Fig. 3, b). During irradiation, a source of ESD origin occurs at some distance from the edges (Fig. 3, c, d). Fig. 3, e, f show that this ESD source is also the area with anomalously high EL output and higher temperature. Coincidence of a location of the local microbreakdown of the cover glass and anomalous EL output with the maximum of temperature distribution along the PVC surface directly indicates that such areas of anomalous EL output at the wavelength of 660 nm are locations of low-resistance shunts between the SP electrodes, which result in additional local heating.

The preliminary study of the role of technological defects of the p-n-junctions of the InGaP/GaAs/Ge-based PVCs has shown that during tests for effect of the electron component of the geomagnetic plasma the anomalously high rate of degradation of the semiconductor photostructure is experienced by the PVCs that initially have substantial defects of the semiconductor structure. Fig. 4 shows the photo images of EL distribution along the area of the adjacent serial PVCs before start of the tests (Fig. 4, a) and at the initial state of the tests after collecting the electron fluence of $1.66 \cdot 10^{14} \,\mathrm{cm}^{-2}$ (Fig. 4, b). During EL excitation, the direct current passing through the PVC before start of the tests was 100 mA at the room temperature, while during the bench tests at the temperature of -47 °C it was 40 mA. It follows from comparing the photo images of these PVCs that the PVC to the right that initially had a substantial technological defect in the InGaP-based p-n-junction (in the form of darkening) was subjected to strong degradation already at the initial stages of the tests.

Let us note that degradation of the operating current that is observed based on the results of the experiment and, therefore, of the PVC power can be explained not only by shunting a part of the operating current. Presence of quite extensive areas of strong shunting indicates significant damage of the PVC semiconductor structure, which can result in degradation of other PVC characteristics, for example, of series resistance or the short-circuit current.

The latter is confirmed by results of preliminary studies of distribution of the short-circuit current in one of the areas of anomalous EL output of the sample N^2 3 (marked by the letter I in Fig. 1). The PVC was covered with an immobile mask of the diameter of 1 mm and to be successively exposed to radiation of photodiodes of the wavelengths of 445, 740 and 940 nm, that excite the p-n- junctions based on InGaP, GaAs and Ge, respectively. The short-circuit current of the element

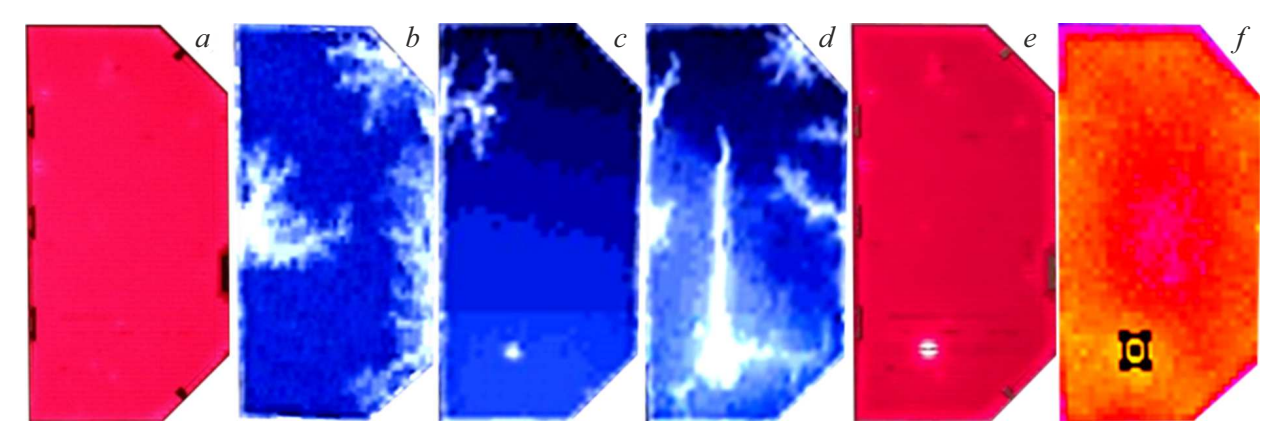


Figure 3. Series of images of the PVC sample under the various conditions: a, e — EL output before and after irradiation by the electron beam, b-d — ESD on the sample surface under irradiation, f — temperature distribution along the PVC surface (the black figure marks the area of the highest temperature).

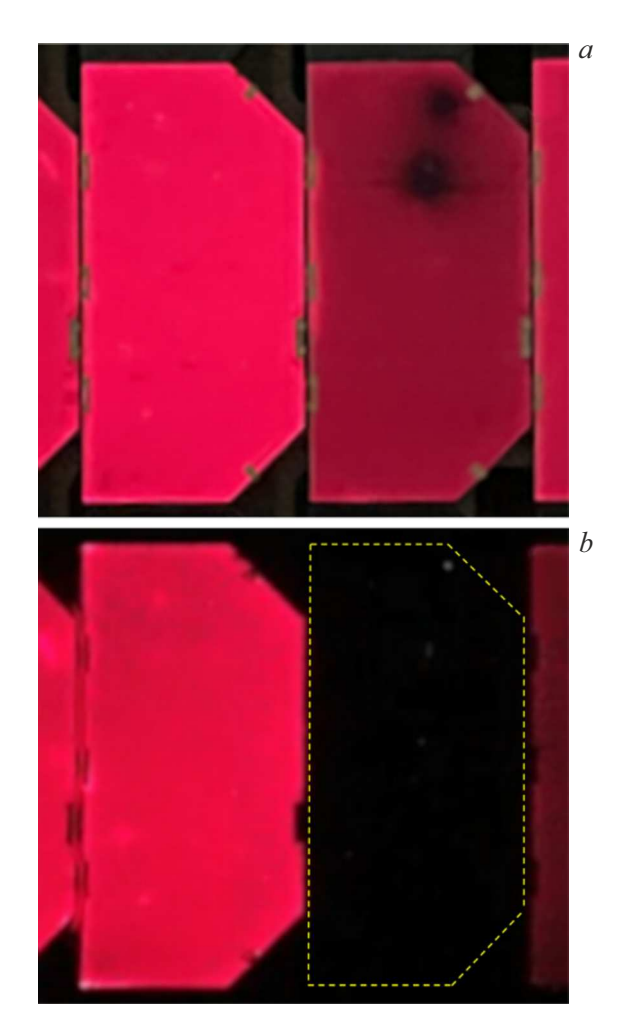


Figure 4. Photo images of PVC EL: a — before irradiation by the electron beam, b — after irradiation.

was recorded by a micro-ammeter and recalculated into the current density taking into account the experiment geometry. The current density distribution along the

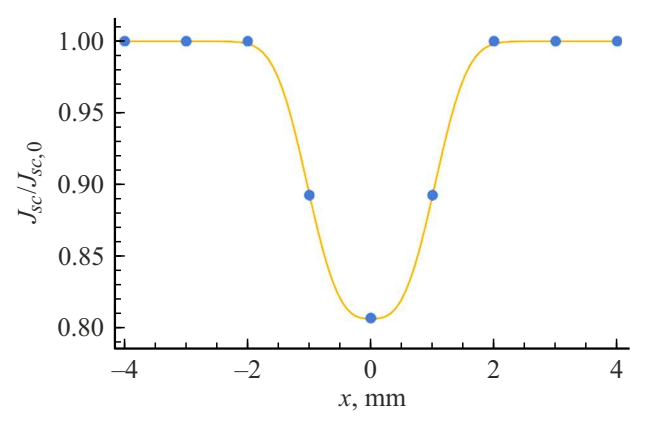


Figure 5. Spatial distribution of the short-circuit current density of the GaAs-based J_{sc} p-n-junction in the damaged PVC are in relation to the current density $J_{sc,0}$ in the undamaged area. The dots — the experimental data, the curve — the approximating line of the trend.

surface was studied by micrometric PVC movement along a direction parallel to the electrodes. The results of measurement of J_{sc} for the GaAs-junction are shown on Fig. 5.

The dependence J_{sc} for the GaAs-junction on the PVC position has a minimum around x=0, which corresponds to a point, in which the maximum EL output was observed at 660 nm. The maximum drop of the short-circuit density in relation to the undamaged area is 19%. The current values for the InGaP- and Ge-junctions were not changed during PVC movement and coincided with the values for the values for the undamaged area. Thus, this area is characterized by degradation of at least two parameters — the shunt resistance and the short-circuit current density for one of the p-n-junction of the element. In general, the issue of degradation of these and other PVC parameters requires additional study.

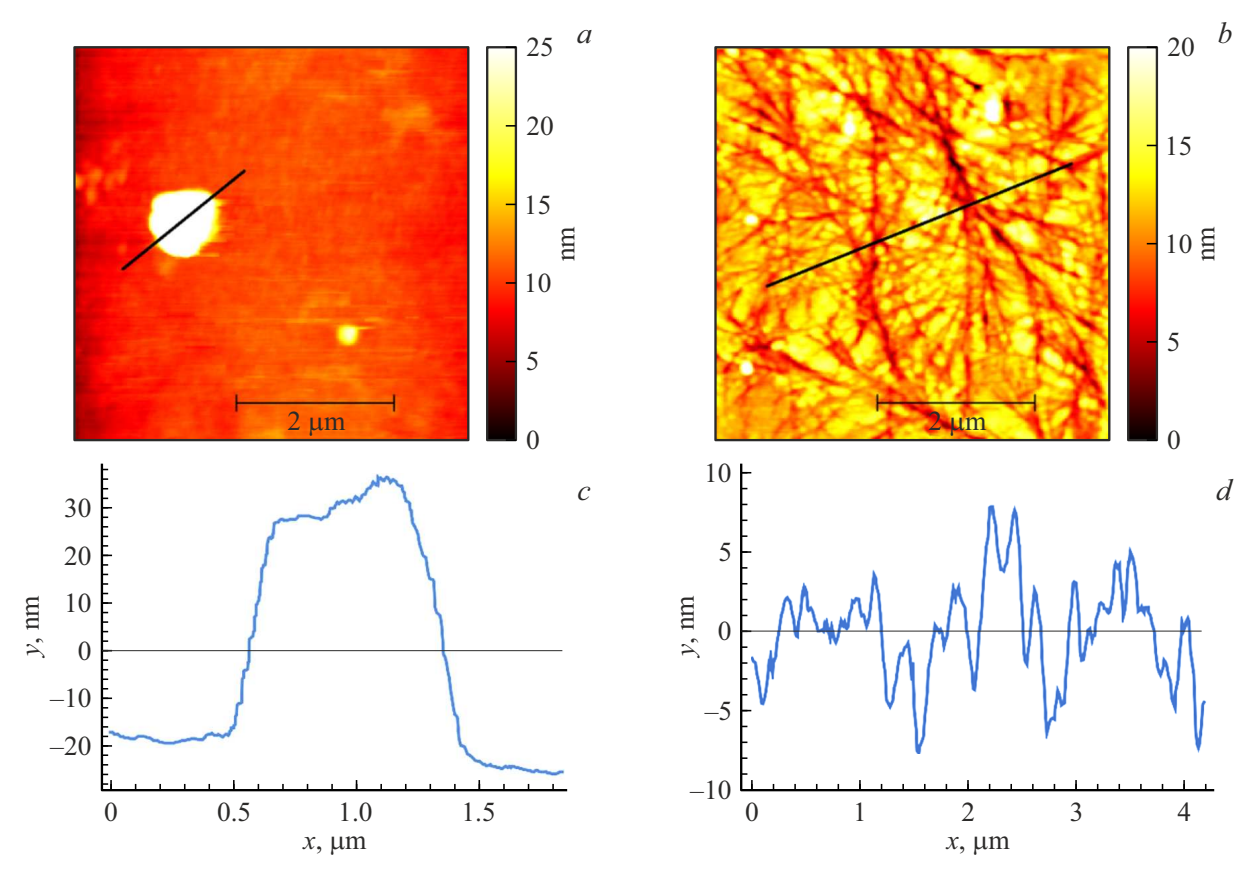


Figure 6. Topography of the surface of the glass sample before irradiation (a, c) and after irradiation (b, d). c — the surface profile along the line on a; d — the surface profile along the line on b.

Study of the nanorelief of the surface of the SP PVC cover glasses by the atomic-force microscopy during laboratory modeling of effect by the geomagnetic plasma electrons

We used the same installation to clarify the causes of origin of the areas of the cover glass microbreakdowns and SP PVC strong shunting in an experiment of irradiating the samples of the cover glasses of the K-208 grade with the sizes 20×20 mm. Each glass sample had across the entire area a rear conductive tantalum coating and a brass cylindrical backgate of the diameter of 10 mm. The coating was applied by magnetron sputtering and had a surface resistance of $100\,\Omega/\Box$. During the exposure the backgate was held at a zero potential. The temperature modes and the cyclogram of effect by the electron beam with the energy of $40\,\mathrm{keV}$ replicate the above-described experiment on the test bench "Prognoz-2".

The surface topography before and after electron irradiation was studied in a contact mode by the atomic-force microscope NT-MDT NTEGRA AURA (Zelenograd, Moscow, the Russian Federation) in air. The experiment used the cantilever NSG01 (NT-MDT, RF)

with the average stiffness of $5.1\,\mathrm{N/m}$ and the typical resonance frequency of $150\,\mathrm{kHz}$. The measurements were performed without additional sampling preparation. The obtained images were processed by the Gwyddion software. The typical results are shown on Fig. 6.

In general, before irradiation the main part of the glass surface is quite smooth. Nevertheless, it has single quite large inhomogeneities with transverse sizes of microns and a height of tens of nanometers, which could be, for example, frozen glass drops. After irradiation, the surface of the cover glass is covered by a network of tree-like electric-discharge channels with a residual depth of 10-20 nm after solidification of glass boiling therein. It is obvious that a part of the substance in the discharge surface channels boils off and splashes to the adjacent glass surface to create new nanometer-scale formations after discharge decay and glass solidification.

Besides, after irradiation, the surface exhibits inhomogeneities shaped as debris with typical sizes of several and tens of microns as well as microcraters of a large depth (presumably, through ones), whereas no such object was observed before irradiation. Presence of such microrelief after irradiation is also confirmed by results of the other authors [14,15].



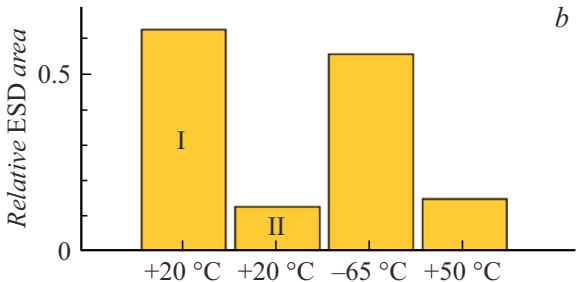


Figure 7. a — the example of the electrostatic discharge, b — comparison of the relative area occupied by the discharges, at the different temperatures. See the text for details of the comparison.

3. Study of electric-discharge phenomena on the surface of the SP PVC cover glasses by video observation during laboratory modeling of effect by the geomagnetic plasma electrons

As noted above, the modeling of effect of the geomagnetic plasma on the SP PVC cover glasses included photovideo recording of the electric-discharge processes. At the initial stage of the experiment, the discharge channels began either on the sample edges or on the cracks of the right upper sample and were tree-like structures. Later on, there were other sources of a discharge beginning. This phenomenon is analyzed below in the text. Fig. 7 exemplifies the ESD picture and compares the relative area occupied by the discharge on the samples at the different temperatures.

At the beginning of the experiment, before the cooling process, the samples of the PVC cover glasses were irradiated at the room temperature $(+20\,^{\circ}\mathrm{C})$. In doing so, there were several strong electrostatic discharges covering a noticeable portion of the area of the glass samples

(Fig. 7, b, I). The average time between the discharges at the room temperature was 14 s. These discharges modified the glass surface so as a discharge afterglow was not only in the form of the network of the discharge channels, but in the form of a set of glowing pointed microformations at surface areas adjacent to the discharge channels (Fig. 7, a). The subsequent discharges on the glass surface at the room temperature covered a significantly lesser area of the samples (Fig. 7, b, II), the discharge frequency increased, and the average time between the discharges was about The relative area of the discharges was probably reduced due to "metallization" of the glass surface by initial discharges owing to electrostatic deposition of positive ions (sodium, potassium, boron and silicon) contained in the electric-discharge plasma of the initial ESDs to the glass surface and subsequent chemisorption thereof.

The main part of the experiment was at the temperature $-65\,^{\circ}$ C. The strength and the frequency of the discharges at the low temperature were noticeably higher than at the room temperature. The average time between the discharges was reduced to 2 s. The final part of the experiment was at the temperature $+50\,^{\circ}$ C. In this case, the surface ESDs were quite weak and they cover a small part of the area (Fig. 7, *b*), whereas some areas of the discharge channels have no glowing.

In general, under effect of the electron beam, there is nonuniform luminescence glowing of all the samples (Fig. 7, a). Over time, the biggest luminescence intensity is reached on some glass edges and cracks. Besides, there are point-like sources of luminescence, which are presumably emission centers of an excessive charge of electrons. Probably, it is manifestation of surface inhomogeneities — production defects and debris (frozen drops) that originated during irradiation. These inhomogeneities shaped as micropoints amplify the electric field and the current of autoelectronic emission into vacuum. Glowing of these object may be related to electroluminescence, whose intensity depends on a value of the current flowing through the micro-point [16].

4. Transformation of "quasi-needle" microdefects of the initial surface of the cover glasses into electron emission centers and then into local glass microbreakdowns — sources of periodic electric discharges

The left bottom glass sample (Fig. 7, a) exhibits the noticeable emission center, which manifests itself as a glowing point and is not a source of the surface discharges. Fig. 8 shows typical cases of its activity or passivity. At the initial stage of the experiment, this centers can be active both without the discharges (Fig. 8, a) and with them (Fig. 8, b), too. Besides, sometimes it does not manifest itself even when the discharge channels pass in its vicinity

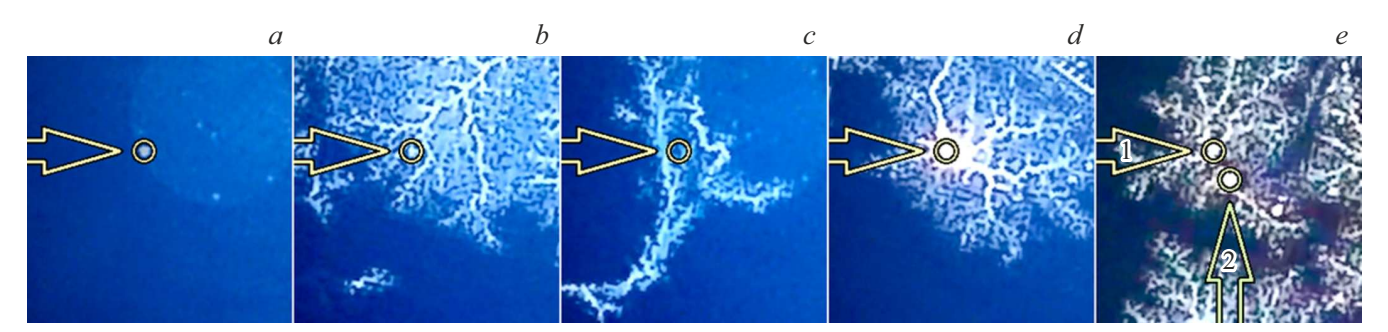


Figure 8. a-d — evolution of activity of the bright emission center at the left bottom sample, e — origination of the second similar center. The center positions are indicated by circles and marked with arrows. The evolution is analyzed in the text.

(Fig. 8, c). Approximately in 30 min after start of irradiation at -65 °C and in 10 s after strong discharge in the vicinity of the said emission center, this center itself becomes a source of ESD beginning (Fig. 8, d).

Apparently, these frames demonstrate consequences of explosion of the emission center with formation of the local glass breakdown. This center is in a location that corresponds to a sharp edge of the brass cylindrical backgate. After transformation (Fig. 8, d), it is a through microbreakdown and together with the sample edges it becomes a constant source of ESD beginning due to formation of a triple point vacuum-dielectric-conductor at the bottom of the microbreakdown. Probability of formation of microbreakdown clusters on the glass surface (that is noted in the study [6,7]) is confirmed by our video observations, when there is formation of another microbreakdown a new source of beginning of ESD (Fig. 8, e) in close vicinity to the above-described microbreakdown. At the temperature of +50 °C, the considered emission centers in the form of glass microbreakdowns become low-activity ones and almost lose a bygone capability of being a source of beginning of the surface discharges.

5. Phenomenological mechanism of anomalous power degradation of the SC SP elements on the orbits with periodic intersection of the Earth's radiation belt

Generalizing the study results, we can presume the following components of the mechanism of anomalous degradation of the PVC power, which with maximum probability manifests itself at the SC orbits with intersection of the radiation belt in the Earth shadow.

– During effect on the PVC by the electron component of the geomagnetic plasma, the surface nanolayer of the cover glass containing large concentration of the structural defects accumulates significant concentration of excessive electrons, while a negative surface potential of the glass increases in magnitude as electrons of the geomagnetic plasma accumulate in the glass.

- Technological microdefects of the surface of the PVC cover glasses, for example, as frozen glass drops are initially the quasi-pointed cathodes which ensure emission of excessive electrons out of the glass into the environment.
- When the surface potential reaches a critical value, there are local electrical breakdowns of the cover glass along a lateral surface.
- The local electrical breakdowns of the cover glass along its lateral surface cause anode-initiated surface discharges of the glass, which refer to discharges with a distributed virtual cathode. The anode-initiated surface discharges are characterized by volume breakdowns of the dielectric's surface nanolayer, which generate plasma in the off-surface layer of vacuum [17].
- Due to quite small values of strength of the electric field (the typical value of potential difference is several kV), the volume breakdown forms a discharge channel, which is filled with boiling glass and partially located in the surface nanolayer of the glass and limited by a boundary of the solid-liquid phase transition, which moves at the subsonic speed towards the virtual cathode.
- In the discharge channel area adjacent to the moving boundary of the phase transition, there is formation of a gaseous phase in the form of bubbles, which grow with evaporation of the liquid phase and can burst resulting in splashing of the micro- and nano-drops to the adjacent glass surface.
- Another part of the anode-initiated surface discharge is formed in the off-surface space as the electric-discharge plasma with the chemical composition of the glass, which creates on the glass surface a conductive layer due to electrostatic deposition of the positive plasma ions such as the ions of silicon, boron, sodium and potassium.
- With quite large probability, alternation of electrostatic deposition of the positive ions from the electric-discharge plasma and splashing of the glass nano-drops to an apex of one of the technological microdefects of the surface of the PVC cover glass can result in formation of a structure in the form of a conductor-dielectric-conductor capacitor.
- With formation of the strong electric field in this capacitor due to electrostatic deposition on it of a large amount of positive ions from the surrounding electric-

discharge plasma from a near surface discharge, explosion destruction of the capacitor may occur. It is known that such phenomena are one of initiators of explosion electron emission [18]. Besides, craters caused by destruction of such nanoscale capacitor can be seen directly [19,20].

- The explosive nano-second destruction of the nano-capacitor at the apex of the technological microdefect forms in the glass a narrow-directional shock wave with a frequency characteristic at the hypersound boundary, which disrupts electrical strength of the glass and causes a glass microbreakdown along its thickness towards the nearest area of the PVC grid electrode.
- In conditions of continuing irradiation by the geomagnetic plasma electrons, the formed through microbreakdown becomes a source of periodic electric discharges with eruption of plasma, a gas and glass particles. These ESDs release a certain part of the external irradiation electron charge accumulated in the glass into the PVC semiconductor structure and generate the shock waves that locally affect the grid electrode, the PVC p-n-junctions and initiate development of a network of the glass cracks.
- The areas with the high density of the microbreakdowns grow under effect of radial cracks of the cover glass in a location of the primary microbreakdowns so that the new microbreakdowns appear in locations where the adjacent grid electrodes are intersected by a separate glass crack.
- Effect of the shock waves that are periodically generated by the electric discharges in the microbreakdowns of the cover glass results in formation of locations of local destruction of the PVC p-n-junctions with redistribution of electric voltage between the junctions depending on their damage degree, thereby resulting in local redistribution of absolute EL output for these p-n-junctions.
- Formation of the locations of low-resistance shunts between the PVC electrodes due to the locations of local destruction of the PVC p-n-junctions by the shock waves that are periodically generated by the discharges in the microbreakdowns seems to result in reduction of the PVC output operating current due to formation of the area of increased series PVC resistance in the vicinity of the microbreakdown.

The work of the above-described mechanism is largely based on high concentration of the charge carriers in the surface nanolayer. It was substantiated by an estimate calculation by the model described in the paper [21] in the conditions similar to the experimental ones when testing the SP and glass samples (Section 1). It follows from analyzing the calculation results that up to 2.5% of the charge introduced by the electron beam in the formed of trap-captured electrons can be concentrated in the surface dielectric layer of the thickness of about 10 nm that contains increased concentration of the defects (the traps of the charge carriers). As we have shown in the paper [21], such high concentration of electrons can be provided in these conditions by generation of trains of optical phonon that are created by each thermalizing electron originated from external irradiation, including the primary beam electrons,

the δ -electrons, etc.Further on, with increase of strength of the electric field in the surface nanolayer, trap ionization due to the Poole-Frenkel effect can result in the I-U curve of the S-type [22,23], overheat-electron instability and development of the volume breakdowns [24] that form the anode-initiated surface discharges.

Another important aspect of the proposed mechanism is that it is possible to damage the semiconductor heterostructure by certain ESD impact. The heterostructure will be the most intensively affected by discharges in its close vicinity, i.e. by the through microbreakdowns and subsequent ESDs inside the already formed channels of such microbreakdowns. Direct mechanical impact and the amplitude of the discharge-created shock wave will be determined by the discharge channel pressure, whose values for various types of the solid dielectrics are estimated to be about $2.5-11\,\mathrm{GPa}$ in case of the micro-second processes and $(6-24)\cdot 10^{10}\,\mathrm{Pa}$ in case of the anode-initiated nanosecond breakdowns [25].

The through microbreakdowns observed in the present study can originate during deposition of the positive ions to the technological defects of the glass and, therefore, they are the anode-initiated ones. That is why the primary microbreakdown can be characterized by quite high pressure in the channel that is compared to Hugoniot elastic limit both of the glass and the semiconductor as well. The value of this parameter for the K-8 glass similar in mechanical properties to the K-208 of the present study is (8 ± 1) GPa [26], and it is (8.4 ± 0.8) GPa for GaAs [27]. Due to proximity of other mechanical constants [28], it can be presumed that the elastic limit of InGaP will be also close to the said values. Thus, the very fact of penetration of the through discharge channel in the glass indicates that direct damage of the semiconductor structure is possible.

As shown by analyzing the video recordings of the test process, the location of the through microbreakdown usually becomes a source of beginning of the periodic surface ESDs. Apparently, these discharges are initiated in the triple point vacuum-dielectric-conductor at the bottom of the microbreakdown and propagate inside the channel and then on the surface. In comparison to the primary microbreakdown, these secondary discharges might be characterized by lesser values of the channel pressure, since the type of these discharges will probably differ from the type of the primary microbreakdown. Nevertheless, the periodic effect of the secondary discharges can also result in degradation of the semiconductor structure similar to the example described in the study [29]. It detected damage of the InGaP/GaAs/Gebased PVC during thermal cycling, which is manifested, inter alia, in growth of cracks in an area where the grid electrodes are adjacent to the semiconductor structure and where stress concentrators originate. Presumably, the primary through microbreakdown results in origination of an initial crack in this area, while the secondary ESDs weaker in effect ensure its growth and further gradual damage of the PVC. Let us note that the PVC semiconductor structure may also be damaged by bombardment of the

charge carriers from the discharge plasma, heating of the grid electrode and the semiconductor by discharge currents and by other factors as well. Further research is needed to clarify significance of these factors and to confirm the entire proposed mechanism of anomalous degradation of the PVC power.

Conclusion

- 1. During the bench tests of the SP samples for effect of the geomagnetic plasma, it has been established that the high initial rate of degradation of the SP operating current (comparable to the initial rate of degradation at the orbits of the GLONASS and GPS navigation systems) can be obtained by modeling the effect of the geomagnetic plasm's electron component taking into account periodic intersection of the Earth's radiation belt by the SC orbit without using the orbit-averaged value of the electron flux density. In these conditions, parameters initiating the initial process of anomalous degradation of the SP power are not integral fluxes (fluences) of electrons and protons, but rather the frequency and the power of electric-discharge processes on the surface of the SP PVC cover glasses, which can be provided by irradiation by an external source of electrons.
- 2. It has been shown by measurements of the I-U curve of some PVCs of the SP sample done by the SP manufacturers after completion of the bench tests with modeling intersection of the Earth's radiation belt that some PVCs are characterized by significant reduction of the operating current (for one of the PVCs the operating current was reduced by 72% with the collected electron fluence of $1.5 \cdot 10^{15}$ cm⁻² with irradiation within the temperature range (from -60 to +50 °C)).
- 3. The dark I-U curves and EL (forward bias) of the test-damaged PVCs have been studied to show that significant shifts of the I-U curves within an operating area were accompanied by origination of local locations of anomalously high EL output in the spectrum red range as well as by formation of areas in the cover glass as the network of the glass cracks and microbreakdowns related thereto.
- 4. By the microscope method with side illumination to control formed glass defects and by the absolute luminescence spectrometry method, it was found that the local locations of anomalously high EL output at the wavelength of 660 nm and anomalously low EL output at the wavelength of 900 nm were at the grid electrode at its both sides and that the location of anomalous EL output necessarily has the microbreakdown of the cover glass along its thickness nearby. Based on measurement of the local short-circuit current density in the vicinity of the locations of anomalously high EL output at the wavelength of 660 nm and anomalously low EL output at the wavelength of 900 nm, it was found that in addition to shunt such a local area had a significantly reduced short-circuit current density. The measured anomalous absolute values of EL output at

the wavelengths 660 and 900 nm unambiguously indicate strong local damage of the GaAs-based p-n-junction with redistribution of voltage between the cascades in favor of the InGaP p-n-junction.

- 5. The special research has been taken on the test bench of the electric-discharge processes on the samples of the K-208 cover glasses, which have a semiconductor structure and the metal electrode as an earthed backgate It was established that when irradiating with electrons of the energy of 30–40 keV and the current density of 10 nA/cm² with great probability the microbreakdowns of the glass along the thickness occurred during the electrical explosion of initial technological microdefects on the glass surface, if these microdefects are located against the edge of the grid electrode, which seems to be a concentrator of the electric field.
- 6. By the additional test for effect of the electron component of the geomagnetic plasma with modeling periodic intersection of the Earth's radiation belt, it was established that the anomalously high rate of degradation was observed for only the PVCs that initially had considerable technological defects of the semiconductor structure, for example, as areas of reduced EL output in the spectrum red range.
- 7. The study has proposed a phenomenological mechanism of anomalous degradation of the SP power on the orbits with periodic intersection of the Earth's radiation belt, which requires confirmation by field experiments. The mechanism is based on the assumption that anomalous degradation of the SP power is due to destruction of the semiconductor photostructure near areas of the grid electrodes, which are adjacent to the microbreakdowns of the cover glass and with SC motion along the orbit subjected to mechanical effect by the shock waves that are periodically generated by electric discharges in the glass microbreakdowns adjacent to them. Local destruction of the semiconductor structure results in local shunting of the PVC p-n-junctions and to local reduction of the shortcircuit current density, probably, due to local increase of series PVC resistance.

Acknowledgments

The authors would like to thank the professor V. I. Korepanov for his help in measuring the electroluminescence spectra, microphotography and recording the short-circuit current.

Funding

In the paper, the equipment of the Centre for Collective Use of the Research and Development Center of the NMNT TPU, supported by the project of the Ministry of Education and Science of Russia N° 075-15-2021-710, was used.

Conflict of interest

The authors declare that they have no conflict of interest.

References

- S.R. Messenger, E.M. Jackson, J.H. Warner, R.J. Walters, T.E. Cayton, Y. Chen, R.W. Friedel, R.M. Kippen, B. Reed. IEEE Trans. Nucl. Sci., 58 (6), 3118 (2011). DOI: 10.1109/TNS.2011.2172957
- [2] D. Ferguson, P. Crabtree, S. White, B. Vayner. J. Spacecraft Rockets, 53 (3), 464 (2016). DOI: 10.2514/1.A33438
- [3] M.I. Panasyuk, L.S. Novikov (red.). Model kosmosa (KDU, M., 2007), t. 2 (in Russian).
- [4] R.H. Khasanshin, L.S. Novikov, S.B. Korovin. J. Surf. Invest.: X-Ray, Synchrotron Neutron Tech., 11, 917 (2017). DOI: 10.1134/S102745101705007X
- [5] R.H. Khasanshin, L.S. Novikov. Inorg. Mater. Appl. Res., 12, 313 (2021). DOI: 10.1134/S2075113321020234
- [6] L.S. Gatsenko, N.E. Maslyakova, M.B. Kagan, L.S. Novikov, M.S. Samokhina. Avtonomnaya energetika: tekhnicheskii progress i ekonomika, (in Russian). 29, 24 (2011).
- [7] N.E. Maslyakova, L.S. Gatsenko, L.S. Novikov, M.S. Samokhina, V.V. Khankin. Tr. Mezhvuzovskoi nauchnoi shkoly molodykh spetsialistov "Kontsentrirovannye potoki energii v kosmicheskoi tekhnike, elektronike, ekologii i meditsine" (M., Rossiya, 2011), s. 105 (in Russian).
- [8] V.E. Skurat, L.S. Gatsenko, A.N. Zhigach, M.B. Kagan, I.O. Leipunsky, L.S. Novikov, P.A. Pshechenkov, V.V. Artemov, N.G. Berezkina. Proc. 12th Int. Symp. On Materials in Space Environment (Noordwijk, Netherlands, 2012)
- [9] C. Gabrielse, J.H. Lee, S. Claudepierre, D. Walker, P. O'Brien, J. Roeder, Y. Lao, J. Grovogui, D.L. Turner, A. Runov, A. Boyd, J. Fennell, J.B. Blake, K. Lopez, Y. Miyoshi, K. Keika, N. Higashio, I. Shinohara, S. Imajo, S. Kurita, T. Mitani. Space Weather, 20, e2022SW003183 (2022). DOI: 10.1029/2022SW003183
- [10] A.M. Vladimirov, A.Yu. Bezhayev, V.M. Zykov, V.I. Isay-chenko, A.A. Lukashchuk, S.E. Lukonin. IOP Conf. Series: Mater. Sci. Eng., 168, 012037 (2017). DOI: 10.1088/1757-899X/168/1/012037
- [11] R. Hoheisel, D. Scheiman, S. Messenger, P. Jenkins, R. Walters. IEEE Trans. Nucl. Sci., 62 (6), 2894 (2015). DOI: 10.1109/TNS.2015.2498838
- [12] J. Janesick, G. Putnam. Annu. Rev. Nucl. Part. Sci., 53, 263 (2003). DOI: 10.1146/annurev.nucl.53.041002.110431
- [13] I. Lombardero, C. Algora. Solar Energy Mater. Solar Cells, 204, 110236 (2020). DOI: 10.1016/j.solmat.2019.110236
- [14] R.H. Khasanshin, L.S. Novikov, S.B. Korovin. J. Surf. Invest.: X-Ray, Synchrotron Neutron Tech., 9, 81 (2015). DOI: 10.1134/S1027451015010115
- [15] R.Kh. Khasanshin, L.S. Novikov, L.S. Gatsenko, Ya.B. Volkova. Perspektivnye materialy, 1, 22 (2015) (in Russian).
- [16] V.V. Serdyuk, Yu.F. Vaksman. *Luministsentsiya poluprovod-nikov* (Vyshcha shk., Kiev-Odessa, 1988) (in Russian).
- [17] W.A. Stygar, J.A. Lott, T.C. Wagoner, V. Anaya, H.C. Harjes, H.C. Ives, Z.R. Wallace, G.R. Mowrer, R.W. Shoup, J.P. Corley, R.A. Anderson, G.E. Vogtlin, M.E. Savage, J.M. Elizondo, B.S. Stoltzfus, D.M. Andercyk, D.L. Fehl, T.F. Jaramillo, D.L. Johnson, D.H. McDaniel, D.A. Muirhead, J.M. Radman, J.J. Ramirez, L.E. Ramirez, R.B. Spielman, K.W. Struve, D.E. Walsh, E.D. Walsh, M.D. Walsh. Phys. Rev. ST Accel. Beams, 8, 050401 (2005). DOI: 10.1103/Phys-RevSTAB.8.050401

- [18] G.A. Mesyats. PMTF, 5, 138 (1980). (in Russian).
- [19] H. Kliem, K. Faliya. IEEE Trans. Diel. El. Ins., 27 (4), 1080 (2020). DOI: 10.1109/TDEI.2020.008526
- [20] J. Muñoz-Gorriz, D. Blachier, G. Reimbold, F. Campabadal, J. Suñé, S. Monaghan, K. Cherkaoui, P.K. Hurley, E. Miranda. IEEE Trans. Dev. Mat. Reliab., 19 (2), 452 (2019). DOI: 10.1109/TDMR.2019.2917138
- [21] V.M. Zykov, D.A. Neyman. Tech. Phys., **68** (6), 690 (2023). DOI: 10.61011/TP.2023.06.56522.21-23
- [22] S. Li, X. Liu, S.K. Nandi, S.K. Nath, R.G. Elliman. Adv. Funct. Mater., 29, 1905060 (2019).
 DOI: 10.1002/adfm.201905060
- [23] A. Pergament, G. Stefanovich, V. Malinenko, A. Velichko. Adv. Cond. Matt. Phys., 2015 (1), 654840 (2015). DOI: 10.1155/2015/654840
- [24] Yu.N. Vershinin. Elektronno-teplovye i detonatsionnye protsessy pri elektricheskom proboe tverdykh dielektrikov (UrO RAN, Ekaterinburg, 2000) (in Russian).
- [25] I.F. Punanov, I.S. Zhidkov, S.O. Cholakh. *Vysokovol'tnyi* nanosekundnyi proboi kondensirovannykh sred: uchebnoye posobiye (Izd-vo Ural'skogo un-ta, Yekaterinburg, 2018) (in Russian).
- [26] A.S. Savinykh, G.I. Kanel, I.A. Cherepanov, S.V. Razorenov. Tech. Phys., 61 (3), 388 (2016).
 DOI: 10.1134/S1063784216030178
- [27] T. Goto, Y. Syono, J. Nakai, Y. Nakagawa. Solid State Commun., 18 (11–12), 1607 (1976). DOI: 10.1016/0038-1098(76)90404-X
- [28] L. Qi, Y. Xie, Y. Liu, H. Jing, R. Zhang. Optik, 198, 163284 (2019). DOI: 10.1016/j.ijleo.2019.163284
- [29] R.E. Brock, P. Hebert, J. Ermer, R.H. Dauskardt. Sol. Energy Mater. Sol. Cells, 179, 178 (2018).
 DOI: 10.1016/j.solmat.2017.11.009

Translated by M.Shevelev